

## ORIGINAL ARTICLE

# Exopolysaccharides from a *Codonopsis pilosula* endophyte activate macrophages and inhibit cancer cell proliferation and migration

Min Chen<sup>1</sup>, Yuanyuan Li<sup>2</sup>, Zhu Liu<sup>2</sup>, Yajun Qu<sup>1</sup>, Huajie Zhang<sup>1</sup>, Dengwen Li<sup>2</sup>, Jun Zhou<sup>2,3</sup>, Songbo Xie<sup>3</sup>  & Min Liu<sup>3</sup> 

<sup>1</sup> State Key Laboratory of Microbial Technology, School of Life Sciences, Collaborative Innovation Center of Cell Biology in Universities of Shandong, Shandong University, Jinan, Shandong, China

<sup>2</sup> State Key Laboratory of Medicinal Chemical Biology, College of Life Sciences, Nankai University, Tianjin, China

<sup>3</sup> Shandong Provincial Key Laboratory of Animal Resistance Biology, Collaborative Innovation Center of Cell Biology in Universities of Shandong, Institute of Biomedical Sciences, College of Life Sciences, Shandong Normal University, Jinan, China

## Keywords

Cancer; *Codonopsis pilosula*; endophyte; exopolysaccharide; macrophage.

## Correspondence

Songbo Xie, College of Life Sciences, Shandong Normal University, 88# Wenhua East Road Jinan, Shandong 250014, China.  
Tel: +86 531 8618 2516  
Fax: +86 531 8618 2518  
Email: xiesongbo@sdsu.edu.cn

Min Liu, College of Life Sciences, Shandong Normal University, 88# Wenhua East Road, Jinan, Shandong 250014, China.  
Tel: +86 531 8618 2516  
Fax: +86 531 8618 2518  
Email: minliu@sdsu.edu.cn

Received: 31 January 2018;  
Accepted: 24 February 2018.

doi: 10.1111/1759-7714.12630

Thoracic Cancer 9 (2018) 630–639

## Abstract

**Background:** Exopolysaccharides with structural diversity have shown wide applications in biomaterial, food, and pharmaceutical industries. Herein, we isolated an endophytic strain, 14-DS-1, from the traditional medicinal plant *Codonopsis pilosula* to elucidate the characteristics and anti-cancer activities of purified exopolysaccharides.

**Methods:** HPLC and GC-MS were conducted to purify and characterize the exopolysaccharides isolated from 14-DS-1. Quantitative RT-PCR, cell migration assays, immunofluorescence staining, and flow cytometry analysis were conducted to investigate the biological activity of DSPS.

**Results:** We demonstrated that exopolysaccharides isolated from 14-DS-1 (DSPS), which were predominately composed of six monosaccharides, showed anti-cancer activities. Biological activity analysis revealed that exposure to DSPS induced macrophage activation and polarization by promoting the production of TNF- $\alpha$  and nitric oxide. Further analysis revealed that DSPS treatment promoted macrophage infiltration, whereas cancer cell migration was suppressed. In addition, DSPS exposure led to S-phase arrest and apoptosis in cancer cells. Immunofluorescence staining revealed that treatment with DSPS resulted in defects in spindle orientation and positioning.

**Conclusion:** These findings thus suggest that DSPS may have promising potential in cancer therapy.

## Introduction

Endophytes are endosymbionts; these organisms, including bacteria and fungi, are ubiquitously found in plants and evolve along with the host plant.<sup>1–4</sup> Endophytes provide the host with many benefits: they can promote growth, contribute to nutrient acquisition, or improve resistance to biotic and abiotic stresses. Endophytes isolated from medicinal plants are reported to be capable of producing the same or similar secondary metabolites as their host plants.<sup>5–10</sup> For example, the endophytic fungus isolated from the yew tree, *Taxusbrevifolia*, can produce the anti-

cancer drug, paclitaxel.<sup>11</sup> *Codonopsis pilosula* is an herbaceous perennial plant mainly grown in China, Japan, and Korea that is widely used in traditional medicine. *C. pilosula* extracts are very complex, consisting of polysaccharides, saponins, sesquiterpenes, polyphenolic glycosides, alkaloids, polyacetylenes, and phytosteroids.<sup>12–14</sup> Polysaccharides isolated from *C. pilosula* are one of the plant's important active constituents, with multiple biological activities, including antioxidant, anti-cancer, and immunomodulatory properties.<sup>15–21</sup> Given that *C. pilosula* endophytes are able to produce similar bioactive molecules as

the plant itself, isolation and identification of *C. pilosula* endophytes could lead to the discovery of novel bioactive molecules.

Microbial polysaccharides, including intracellular polysaccharides, capsular polysaccharides, and exopolysaccharides (EPSs), are natural macromolecules abundant in microorganisms that are important for the maintenance of cell wall integrity and for the regulation of host-pathogen interactions.<sup>22,23</sup> EPSs secreted by microorganisms into the extracellular environment are structurally diverse, allowing for a variety of potential applications in the biomaterial and pharmaceutical industries. A growing body of evidence has revealed that microbial EPSs are beneficial to human health; they show promising activities, including immunomodulation and cytotoxic effects against cancer cells.<sup>24–29</sup> Importantly, emerging studies have revealed that the structural units of the EPS not only determine its function, but the ecological niches of the host microorganism also contribute to EPS activity.<sup>30–37</sup> For example, EPS produced by *Paenibacillus polymyxa*, a bacterium isolated from *Stemona japonica* (Blume) Miquel, exhibited robust scavenging activities for superoxide and hydroxyl radicals.<sup>5</sup> Thus, isolating and characterizing novel EPSs from medicinal plants may lead to the identification of promising biological macromolecules. In this study, we sought to isolate endophytes from the root of *C. pilosula* and to elucidate the characteristics and anti-cancer activities of purified EPSs.

## Methods

### Chemicals and antibodies

All chemicals were purchased from Sigma-Aldrich (St. Louis, MO, USA). Fluorescein isothiocyanate (FITC)-conjugated phalloidin was obtained from ThermoFisher Scientific (Waltham, MA, USA). Antibodies against  $\alpha$ -tubulin and  $\gamma$ -tubulin were obtained from Santa Cruz Biotechnology Inc. (Santa Cruz, CA, USA). Rhodamine or fluorescein-conjugated secondary antibodies were purchased from Jackson ImmunoResearch Laboratories (West Grove, PA, USA). The annexin V-FITC/PI apoptosis detection kit used was obtained from Sigma-Aldrich. Transwell inserts were obtained from BD Biosciences (San Jose, CA, USA).

### Cell culture and treatment

RAW264.7 macrophages, BT549 and MDA-MB-231 breast cancer cells, and HeLa cervical cancer cells were obtained from American Type Culture Collection (Rockville, MD, USA) and cultured in medium as described previously.<sup>38</sup> Cells were maintained at 37°C in a humidified incubator containing 5% CO<sub>2</sub>. Various concentrations of exopolysaccharides

isolated from 14-DS-1 (DSPS) were added to cell culture medium for the indicated times.

### Isolation of endophytes from *C. pilosula*

Fresh *C. pilosula* roots were washed several times under running tap water and sterilized with 75% ethanol for 20 seconds and then with 2.5% sodium hypochlorite for five minutes. *C. pilosula* roots were cut vertically into small segments to expose the inner surface and then inoculated on agar plates. Plates were incubated at 37°C for 48 hours to promote endophyte growth.<sup>39</sup> Each endophytic culture was checked for purity and transferred to freshly prepared agar plates. Appropriate controls were also set up in which no plant tissues were inoculated.

### Physiological characteristics and phylogenetic relationship determination

The physiological characteristics of the isolated strain 14-DS-1 were characterized according to the procedures outlined in Bergey's Manual of Systematic Bacteriology.<sup>40</sup> In brief, 16S rDNA from the 14-DS-1 strain was sequenced, followed by analysis with the BLASTn program (<https://blast.ncbi.nlm.nih.gov/Blast.cgi>). To analyze the phylogenetic relationship, a neighbor-joining phylogenetic tree was constructed using the CLUSTAL program (<http://www.genome.jp/tools-bin/clustalw>), as previously described.<sup>41–43</sup> The defined strain 14-DS-1 was deposited in the China General Microbiological Culture Collection Center.

### Extraction and purification of exopolysaccharides (EPSs) from *C. pilosula* endophytes

The 14-DS-1 strain was cultured in Luria-Bertani liquid medium and agitated at 37°C for 48 hours. The biomass of the bacteria was removed by centrifugation at 5000 rpm for 10 minutes, and then the cell-free supernatants were treated once with Sevag reagent (Sinopharm, Shanghai, China) to remove free protein at 4°C overnight. The volume ratio of the supernatants and Sevag reagent was 4:1, while chloroform and butanol was 5:1. Samples were clarified by centrifugation at 8000 rpm for 15 minutes, and the supernatants were treated with 10% ethanol (v/v) at 4°C overnight. The following day, the samples underwent centrifugation at 10000 rpm at 4°C for 30 minutes. A crude EPS sample was then dissolved in deionized water. The EPS solution was loaded onto a Sephadex G-50 flow column (16 × 100 cm; Sigma-Aldrich) and eluted with deionized water. Only one major fraction was detected, and the collected fraction was termed DSPS.

## Molecular weight determination

The molecular weight of DSPS was determined by high performance liquid chromatography. Size-exclusion chromatographic (SEC) separation was carried out using a Shodex 803 column connected to a Waters model 515 HPLC system (Waters, Rydalmere NSW, Australia) coupled to a refractive index detector (Wyatt-OptilabrEX) and a Wyatt-DAWN HELEOS-II laser light scattering spectrometer (Wyatt Technology Corporation, Santa Barbara, CA, USA).

## Monosaccharide composition analysis

The purified polysaccharide sample (2 mg) was hydrolyzed with 2 mL of 2 M trifluoroacetic acid at 110°C for 1.5 hours. After hydrolysis, the solution was evaporated to dryness at 50°C, and then a stream of methanol (3 mL) was used to remove the excess acid. This procedure was repeated five times. Sodium borohydride (60 mg) was then added to obtain the reducing reaction at room temperature for eight hours. Several drops of glacial acetic acid were added to stop the reaction. The solution was then evaporated to dryness at 50°C. Methanol (3 mL) was used to remove the reducing agent five times, and then the residue was dried at 110°C for 15 minutes. Acetylation was performed using acetic anhydride (3 mL) and pyridine (1 mL) at 100°C for five hours. The mixture was then evaporated to dryness and trichloromethane (5 mL) was added to dissolve the residue. The organic phase consisted of washing with distilled water (2 mL) four times to remove impurities. Finally, the water was removed with anhydrous sodium sulfate and the mixture was transferred into a vial for gas chromatography-mass spectrometer (GC-MS) (Agilent Technologies, Santa Clara, CA, USA) analysis. The GC-MS was used to separate the monosaccharides. A capillary column Hp-5 (Agilent 19091J-413) (30 m × 0.25 mm × 320 μm) was used, with 30.0 mL/min for hydrogen, 400.0 mL/min for air, and with helium as carrier gas at a constant flow of 1 mL/min. The temperature program was set as: initial temperature 120°C, 3°C/min ramp to 250°C, and held for five minutes. The total duration of analysis was 35 minutes. The temperature of the injection port was 250°C and a 1 μL volume was injected in splitless mode.

## Quantitative reverse transcriptase-PCR

Quantitative reverse transcriptase-PCR (RT-PCR) assay was performed as previously described.<sup>44,45</sup> Briefly, total RNA was extracted using Trizol reagent (Invitrogen, Carlsbad, CA, USA) according to the manufacturer's instructions. RNA was reverse transcribed to complementary DNA using a reverse transcription PCR Purification kit (Promega, Madison, WI, USA). TNF-α messenger RNA

expression was evaluated by quantitative RT-PCR (TNF-α primers: 5'-CCCAAAGGGATGAGAAGTTCCCAAAT-3' and 5'-CCACTTGGTGGTTTGCTACGACG-3'; β-actin primers: 5'-CAGAAGGAGATTACTGCTCTGGCT-3', and 5'-TACTCCTGCTTGCTGATCCACATC-3').

## Quantification of nitric oxide production

Nitric oxide (NO) production was examined as previously described.<sup>46</sup> In brief, RAW264.7 cells were treated with various concentrations of DSPS for 24 hours. NO production was estimated by measuring nitrite levels in cell supernatants with Greiss reagent (1% sulfanilamide, 0.1% naphthyl ethyl diamine dihydrochloride, 2.5% phosphoric acid; Sigma-Aldrich). Absorbance was read at 540 nm, and NaNO<sub>2</sub> was used as a standard to quantify NO production.

## Cell migration assays

For transwell migration assay (BD Biosciences), RAW264.7 cells resuspended in serum-free medium were pretreated with various concentrations of DSPS. Cells were then added to insert chambers and incubated for 16 hours. Cells on the upper surface of the inserts were completely wiped off with a cotton swab, while cells that migrated to the underside of the inserts were fixed with 4% paraformaldehyde for 15 minutes at room temperature. Cells were then stained with 0.5% crystal violet in 20% methanol for 30 minutes, washed three times with distilled water, and visualized with a Leica stereomicroscope (Leica Microsystems, Wetzlar, Germany).<sup>47,48</sup> For wound healing assay, cells were grown to 90% confluence in a 12-well plate, and a scratch wound was created in the monolayer using a pipette tip. Cell debris was removed by washing three times with phosphate-buffered saline (PBS). Cells were incubated in complete culture medium for the indicated times to allow wound healing. Phase-contrast images of the wound were captured at the indicated time points.

## Fluorescence microscopy

Cells were fixed with 4% paraformaldehyde for 20 minutes, permeabilized with 0.05% Triton X-100 (Sigma-Aldrich) in PBS for 30 minutes, and blocked with 2.5% bovine serum albumin for one hour at room temperature. Cells were then sequentially incubated with the indicated primary and secondary antibodies, followed by staining with 4',6-diamidino-2-phenylindole. Coverslips were mounted with 90% glycerol and visualized with a Leica TCS SP8 confocal microscope (Leica Microsystems). The spindle angle and positioning were determined as previously described.<sup>49–51</sup>

## Fluorescence-activated cell sorting analysis

Cell cycle progression and apoptosis analysis were performed as previously described.<sup>52</sup> In brief, cells were collected and washed twice with ice cold PBS, and then fixed with 70% ethanol. Cell suspensions were clarified by centrifugation at  $1000 \times g$  for 10 minutes, and the pellets were resuspended in phosphate/citrate buffer (pH 7.5) for 30 minutes. To analyze cell cycle progression, cells were washed with PBS and stained with propidium iodide (PI) for 30 minutes. To analyze apoptosis, cells were stained with Annexin V-FITC/PI for 15 minutes using the Annexin V-FITC/PI Apoptosis Detection Kit (Sigma-Aldrich). Samples were analyzed using a flow cytometer (BD Accuri C6 Plus, BD Biosciences).

## Results

### Strain isolation and biochemical and molecular characterization of 14-DS-1

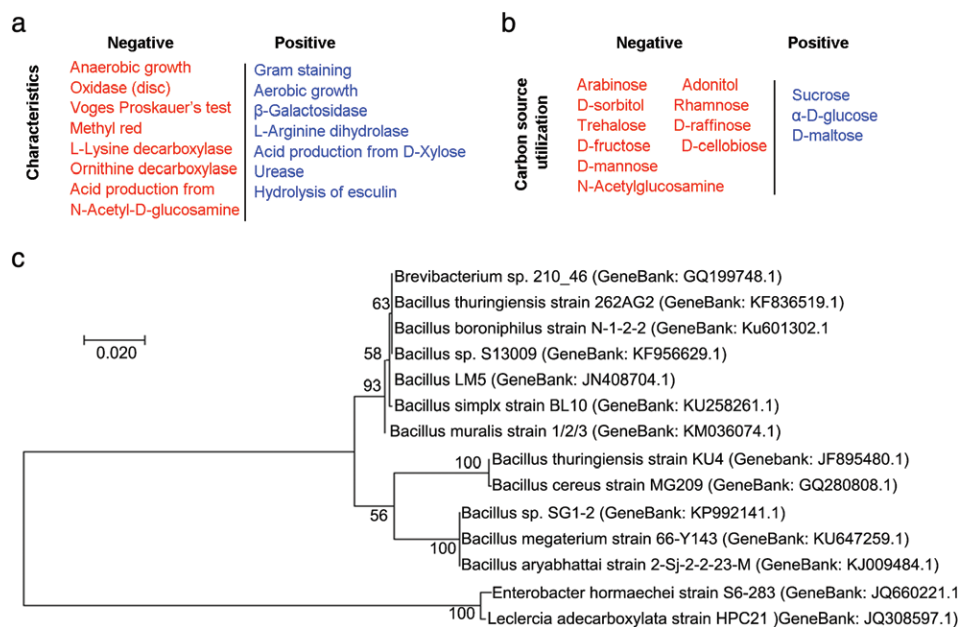
To isolate and identify endophytes capable of producing bioactive molecules, we collected fresh *C. pilosula* root tissue and successfully isolated a strain, 14-DS-1, which was capable of producing EPSs. Characterization of this strain revealed that 14-DS-1 is an aerobic, gram-positive bacterium that utilizes sucrose, glucose, and maltose as carbon sources (Fig 1a,b). We then analyzed the phylogeny of this strain by 16S rDNA sequencing. The 16S rDNA gene sequences of 14-DS-1 (GenBank accession number:

KY658460) were amplified by PCR, sequenced, and compared to all sequences in GenBank. The 14-DS-1 strain belonged to a sub-branch of the genus *Bacillus*, *Bacillus aryabhatai*; based on sequence alignment, 14-DS-1 is 99% similar to this strain. To elucidate the evolutionary relationship, we constructed a phylogenetic tree using the neighbor-joining method. We found that 14-DS-1 is the closest match to *Bacillus* sp., a genus that includes the *Bacillus* sp. SG1-2, *Bacillus megaterium*, and *Bacillus aryabhatai* strains, with 98% similarity (Fig 1c).

### Characterization of EPSs purified from 14-DS-1

As EPSs constitute the major active biomolecule produced by endophytic bacteria, we next isolated and purified EPSs from 14-DS-1. The deproteinized and decolorized constituents secreted by 14-DS-1 contained ~32% EPSs. The crude EPSs were further purified by Sephadex G-50 flow column chromatography (Sigma-Aldrich). Only one fraction was obtained, which was named DSPS (Fig 2a). The molecular weight of DSPS was determined using a Wyatt-DAWN HELEOS-II laser light scattering spectrometer (Wyatt Technology Corporation), and the molecular weight was found to be  $1.68 \times 10^4$  Da (data not shown). The monosaccharide composition of DSPS was analyzed by GC-MS, revealing that it is mainly composed of galactose and glucose, as well as rhamnose, fucose, arabinose, and mannose (Fig 2b). Additionally, we obtained the infrared spectrum of DSPS (Fig 2c).

**Figure 1** Determination of the physiological characteristics and phylogenetic relationships of the isolated strain. (a) Characteristics of the endophytic strain 14-DS-1 isolated from *Codonopsis pilosula*. (b) Carbon-source utilization analysis of the strain 14-DS-1. (c) Neighbor-joining phylogenetic relationship analysis based on 16S rDNA sequencing. Genbank accession numbers are annotated in parentheses. Scale bars, 0.02 substitutions per nucleotide position.



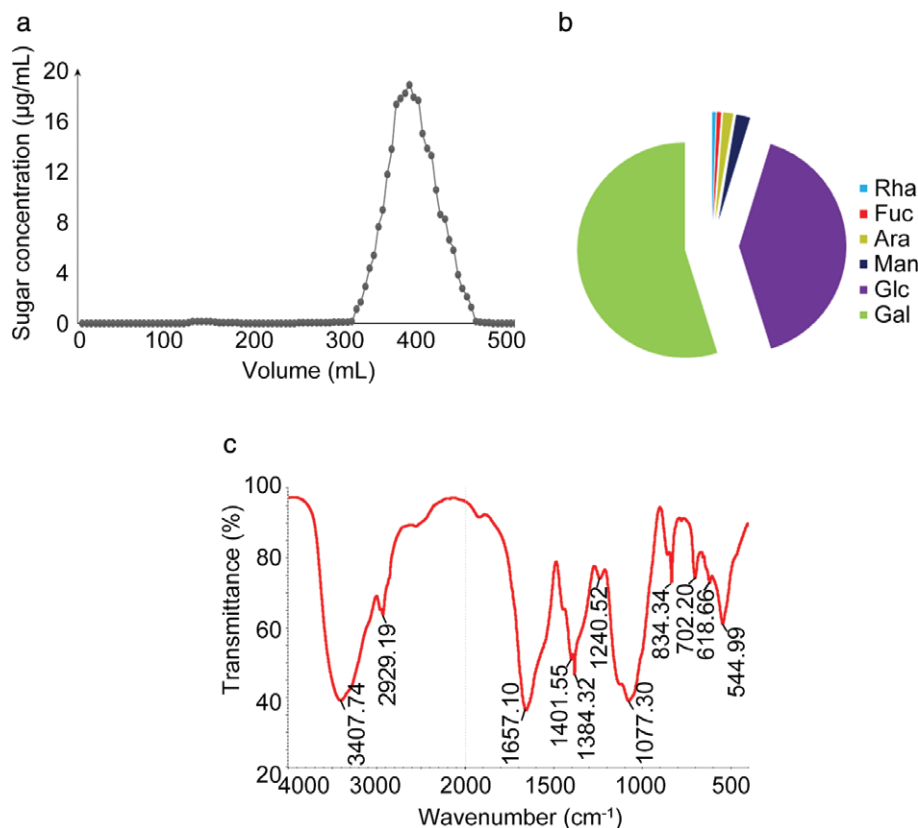


**Figure 2** Characterization of DSPS purified from the strain 14-DS-1. (a) Exopolysaccharides were isolated using a Sephadex G-50 flow column. (b) Analysis of the monosaccharide composition of DSPS. Rha, Fuc, Ara, Man, Glc, Gal. (c) The infrared spectrum of DSPS.

### DSPS promotes macrophage polarization toward the classically activated macrophage (M1) phenotype

As the primary phagocytic cell type, macrophages are activated to phagocytose foreign cells and cellular debris.<sup>53</sup> We investigated the effect of DSPS on macrophage activation in RAW264.7 cells. Activated macrophages undergo morphological transformation, changing from round-shaped cells to flattened spreading cells with pseudopodium-like protrusions. We found that in the control cells and those treated with low concentrations of DSPS, cells remained round; however, exposure to a higher concentration of DSPS (5 mg/mL) led to macrophage activation, as evidenced by an elongated morphology in appropriately 25% of cells (Fig 3a,b). Macrophages can be polarized toward an anti-cancer, M1, or alternatively, pro-tumor, M2, phenotype, depending on the stimuli. To determine the role of DSPS in macrophage activation, we analyzed the production of inflammatory mediators, TNF- $\alpha$  and NO, both of which are secreted by the M1 macrophage subset.<sup>54</sup> We found that higher concentrations of DSPS significantly elevated the production of TNF- $\alpha$  and NO, indicating a critical role of DSPS in promoting polarization of macrophages to the M1 phenotype (Fig 3c,d). This result may provide valuable information for the development of

macrophage-mediated immune therapy for cancer treatment.

### DSPS plays roles in the differentiation and migration of macrophages and in cancer cell migration

As macrophage infiltration to the site of tumors is a prerequisite for macrophages to inhibit tumor progression, we explored the regulatory role of DSPS in macrophage migration. RAW264.7 cells were treated with different concentrations of DSPS, and cell migration was analyzed using a transwell assay. We found that high concentration of DSPS (1 mg/mL and 5 mg/mL) significantly promoted RAW264.7 cell migration across the permeable membrane (Fig 4a,b).

To investigate the underlying mechanism of the DSPS mediated enhancement of macrophage migration, we analyzed the effect of DSPS on the formation of filopodia: actin-rich membrane protrusions critical for cell adhesion and migration. Immunostaining of F-actin revealed that high concentrations of DSPS led to an increase in filopodia formation (Fig 4c,d), suggesting a role of DSPS in filopodium-mediated macrophage migration. Additionally, we investigated the effect of DSPS on cancer cell migration. In contrast to the results observed in macrophages, DSPS remarkably repressed the

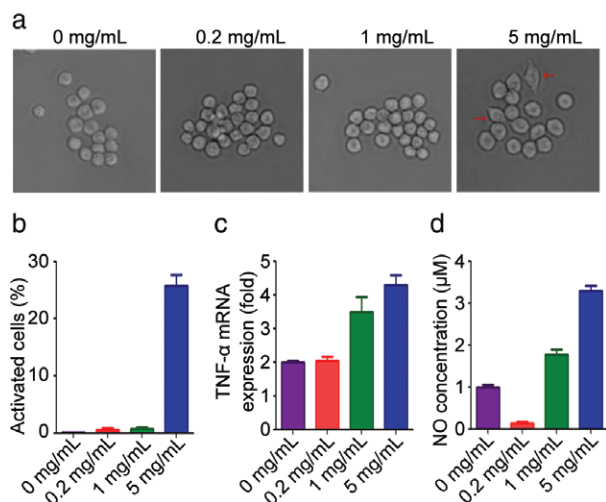


**Figure 3** DSPS activates macrophages. (a) RAW264.7 cells were treated with various concentrations of DSPS for 24 hours, and the cellular morphology was analyzed with a phase-contrast microscope. (b) Quantification of activated macrophages for experiments performed as described in (a). (c) Quantitative reverse transcriptase-PCR analysis of the relative expression of TNF- $\alpha$  messenger RNA (mRNA). (d) Quantification of nitric oxide (NO) production by RAW264.7 cells.

migration of BT549 and MDA-MB-231 breast cancer cells (Fig 4e,f), suggesting its potential as an inhibitor of tumor metastasis.

### DSPS affects cell cycle progression and promotes apoptosis of cancer cells

To further investigate the anti-cancer properties of DSPS, we analyzed its effect on cell cycle progression. MDA-MB-231 cells treated with various concentrations of DSPS were stained with 4',6-diamidino-2-phenylindole and analyzed by flow cytometry. Treatment with DSPS (5 mg/mL) resulted in an increase in S phase cells and a decline in G2/M cells, indicating that DSPS inhibits the DNA replication process (Fig 5a,b).

Next, we sought to determine whether DSPS treatment could induce cell death. Using Annexin V-FITC/PI staining, we found that treatment with DSPS (5 mg/mL) remarkably increased the percentage of apoptotic cells, including cells in both early and late stages of apoptosis (Fig 5c–f). Collectively, these data suggest a promising anti-proliferative role of DSPS in the treatment of cancer cells.

### DSPS affects spindle orientation and positioning in cancer cells

As spindle orientation is essential for proper cell division and cell fate determination, we investigated the effect of

DSPS on this process. Immunofluorescence microscopy revealed that DSPS treatment increased the z-value between the bipolar spindles without affecting the overall morphology or spindle length (Fig 6a,b); this change resulted in an increase in the spindle angle (Fig 6a–c). Next, we measured the distance between the cell center and the spindle center to determine the effect of DSPS on spindle positioning (Fig 6d). Exposure to DSPS (5 mg/mL) significantly increased the distance between the cell center and the spindle center, suggesting a spindle-positioning defect (Fig 6e,f). Taken together, these data reveal a critical role of DSPS in the regulation of spindle orientation and positioning.

## Discussion

*C. pilosula* is a traditional medicinal plant with promising anti-cancer activity. However, little progress has been made in isolating and identifying endophytes from this plant capable of producing active secondary metabolites.<sup>45,55–57</sup> In this study, we isolated an endophyte strain, 14-DS-1, characterized its phylogenetic relationships, and analyzed its physiological properties. Importantly, our study revealed that EPS is the predominant component of 14-DS-1 extracts, and DSPS, as its active ingredient, exhibits

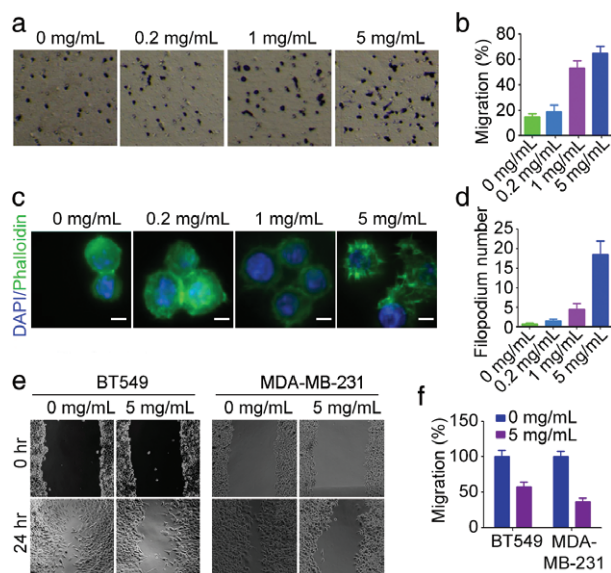


**Figure 4** DSPS affects cell migration. (a) Transwell migration assay showing the effect of DSPS treatment on RAW264.7 cell migration. (b) Quantification of cell migration; cells were treated as in panel (a). (c) Immunofluorescence staining of actin (fluorescein isothiocyanate-conjugated phalloidin) and nuclei (4', 6-diamidino-2-phenylindole) in RAW264.7 cells. Scale bars, 5  $\mu$ m. (d) Quantification of filopodia presented in panel (c). (e) Representative wound healing assay analyzing the effects of DSPS on the migration of BT549 and MDA-MB-231 breast cancer cells. (f) Quantification of migrated cells treated as in panel (e).

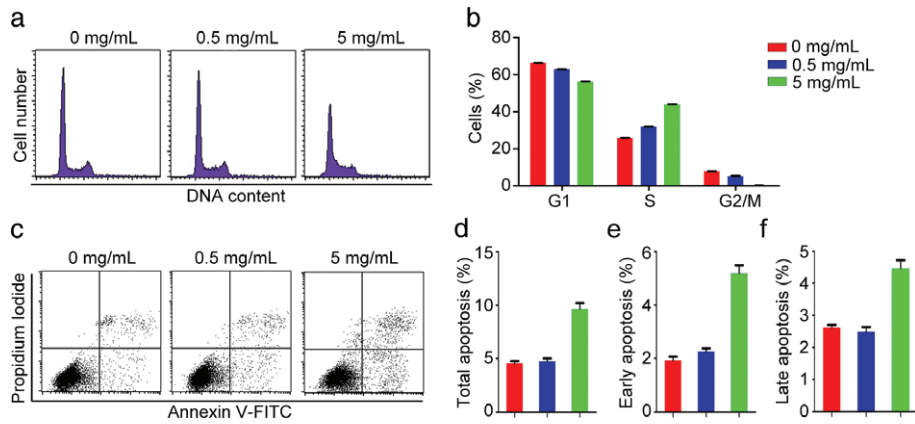


**Figure 5** DSPS alters cell cycle progression and promotes apoptosis. (a) MDA-MB-231 cells treated with various concentrations of DSPS were stained with PI, and the cells were analyzed by flow cytometry to determine cell cycle progression. (b) Quantification of the percentage of cells in G1, S, and G2/M phases of cells treated as in panel A. 0 mg/mL, 0.5 mg/mL, 5 mg/mL. (c–f) MDA-MB-231 cells treated with various concentrations of DSPS and stained with Annexin V fluorescein isothiocyanate (FITC)/propidium iodide (c); the percentage of total apoptotic cells (d), cells in early apoptosis (e), and cells in late apoptosis (f) were quantified.

promising immunoregulatory and anti-cancer properties. EPSs, which are composed of repeating units of sugars or sugar derivatives, can be grouped into homopolysaccharides or heteropolysaccharides, depending on their

monosaccharide compositions.<sup>45,58–61</sup> Our analysis revealed that DSPS is a heteropolysaccharide comprising six monosaccharides. EPSs produced by endophytes are strain-dependent, and their structural and compositional diversity

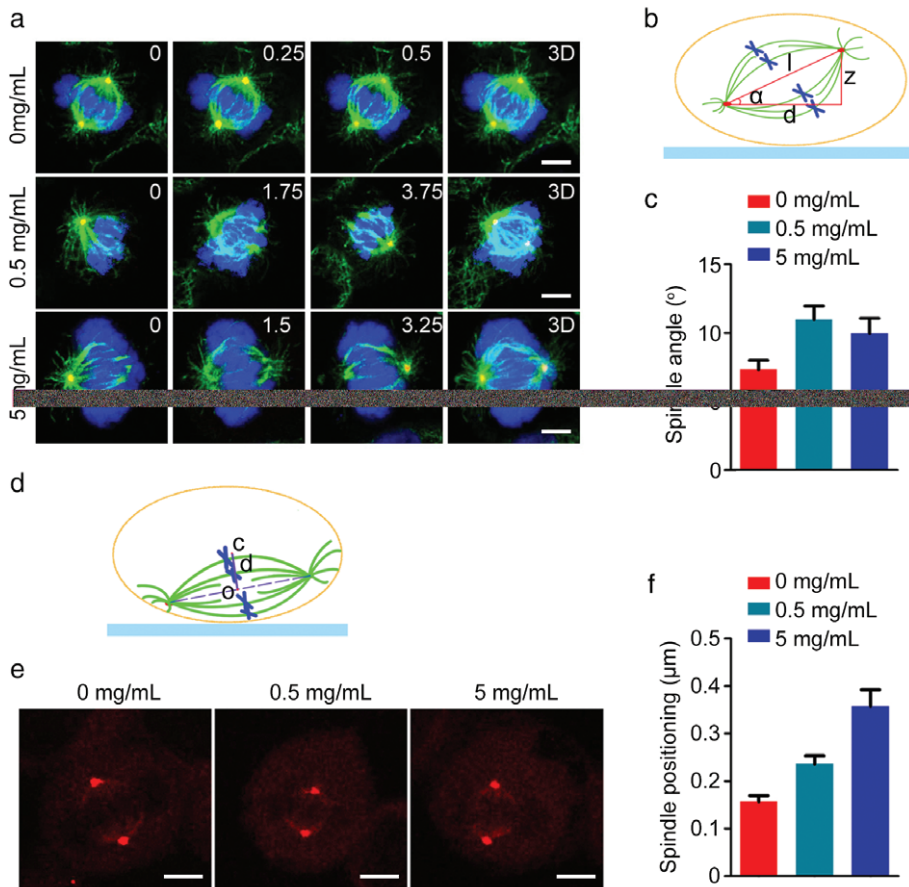


**Figure 6** DSPS impairs spindle orientation and positioning. (a) HeLa cells treated with various concentrations of DSPS were stained with  $\alpha$ -tubulin (green) and  $\gamma$ -tubulin (red) antibodies and 4', 6-diamidino-2-phenylindole (blue). The position of the z stage is indicated in micrometers; 3D, xy projection. Scale bars, 5  $\mu$ m. (b) A diagram illustrating the spindle angle ( $\alpha$ ) measurement. (c) Determination of average spindle angle of cells treated as in panel (a). 0 mg/mL, 0.5 mg/mL, 5 mg/mL. (d) A diagram illustrating the distance (d) between the cell center (c) and the spindle center (o). (e) HeLa cells treated with DSPS were immunostained with  $\gamma$ -tubulin to visualize spindle poles. Scale bars, 5  $\mu$ m. (f) Quantification of the distance between the cell center and the spindle center. 0 mg/mL, 0.5 mg/mL, 5 mg/mL.

conveys unique and varied biological activities.<sup>31,44,62–64</sup> Given that endophytes can be grown in large-scale cultures, have a short growth period, and are easily isolated, the 14-DS-1 strain isolated in this study may have great potential for future applications.

Because of their role in phagocytosis and antigen presentation, macrophages are critical for cancer immunosurveillance.<sup>65–68</sup> Macrophage activation and infiltration in response to inflammation is important for macrophage-related immunosurveillance. Our data demonstrate that DSPS promotes macrophage activation and migration, suggesting an immunomodulatory function for this EPS. While macrophages are important to inhibit tumor development, a growing body of evidence demonstrates that cancer cells can foster macrophages present in the tumor microenvironment to promote tumor growth.<sup>69–71</sup> Specifically, macrophages play distinct roles in cancer progression depending on their polarized phenotype.<sup>72</sup> Classically activated macrophages (M1) suppress tumor growth, metastasis, and angiogenesis. However, in response to the tumor microenvironment, M1 cells can be induced to become alternatively polarized M2 cells, a change that facilitates the escape of cancer cells from immune surveillance. M1 and M2 subtypes can be shifted reversibly in response to different environmental stimuli.<sup>67,72,73</sup> Therefore, identification of biological molecules that can repolarize the tumor-promoting M2 cells into anti-cancer M1 subsets would be of therapeutic value for the treatment of cancer. Importantly, we revealed that DSPS isolated from 14-DS-1 enhances the production of TNF- $\alpha$  and NO, inflammatory mediators secreted by anti-cancer M1 subsets,<sup>74–76</sup> suggesting a potential application for this molecule in cancer treatment.

Further analysis revealed that treatment with DSPS also increased macrophage migration; in contrast, cancer cell migration was inhibited by this polysaccharide. However, the molecular mechanism underlying the role of DSPS in cell migration remains to be elucidated. Additionally, we found that exposure to DSPS resulted in synthesis phase (S phase) cell cycle arrest and apoptosis of cancer cells, demonstrating its anti-cancer activity. Furthermore, our data demonstrate that treatment with DSPS resulted in impaired spindle orientation and positioning, events critical for proper cell division and cell fate determination.<sup>50,51</sup> Given that inappropriate cell division can affect cell cycle progression and initiate apoptotic cell death, DSPS-induced defects in spindle orientation and positioning suggest a mechanism for the anti-cancer effect of this molecule, underscoring its potential for use in cancer therapy.

## Acknowledgments

This work was supported by grants from the National Natural Science Foundation of China (31741039, 31701216,

and 31770997), the Natural Science Foundation of Shandong Province (ZR2017MC008), and the China Postdoctoral Science Foundation (2016M600553).

## Disclosure

No authors report any conflict of interest.

## References

- 1 Abdalla MA, Matasyoh JC. Endophytes as producers of peptides: An overview about the recently discovered peptides from endophytic microbes. *Nat Prod Bioprospect* 2014; **4**: 257–70.
- 2 Nair DN, Padmavathy S. Impact of endophytic microorganisms on plants, environment and humans. *Sci World J* 2014; **2014**: 250693.
- 3 Wang CM, An LG, Huang Y. Two new species of Terschellingia (Nematoda: Monhysterida: Linhomoeidae) from the East China Sea. *Cah Biol Mar* 2017; **58**: 33–41.
- 4 Yang HT, Zou SS, Zhai LJ *et al.* Pathogen invasion changes the intestinal microbiota composition and induces innate immune responses in the zebrafish intestine. *Fish Shellfish Immunol* 2017; **71**: 35–42.
- 5 Liu J, Luo JG, Ye H, Sun Y, Lu ZX, Zeng XX. Production, characterization and antioxidant activities in vitro of exopolysaccharides from endophytic bacterium *Paenibacillus polymyxa* EJS-3. *Carbohydr Polym* 2009; **78**: 275–81.
- 6 Zheng LP, Zou T, Ma YJ, Wang JW, Zhang YQ. Antioxidant and DNA damage protecting activity of exopolysaccharides from the endophytic bacterium *Bacillus cereus* SZ1. *Molecules* 2016; **21**: pii: E174.
- 7 Lü L, Zhao ZT. *Lecanora shangrilaensis* sp nov., on pinecones from China. *Mycotaxon* 2017; **132**: 441–4.
- 8 Wang WC, Zhao ZT, Zhang LL. Four new records of *Rhizocarpon* from China. *Mycotaxon* 2015; **130**: 739–47.
- 9 Zhao X, Zhang LL, Sun LY, Hu L, Zhao ZT. Four new records of *Lecanoraceae* in China. *Mycotaxon* 2015; **130**: 707–15.
- 10 Zhao XX, Zhao ZT, Miao CC, Ren ZJ, Zhang LL. Five *Lecidea* lichens new to China. *Mycotaxon* 2017; **132**: 317–26.
- 11 Xie S, Zhou J. Harnessing plant biodiversity for the discovery of novel anticancer drugs targeting microtubules. *Front Plant Sci* 2017; **8**: 720.
- 12 Mizutani K, Yuda M, Tanaka O *et al.* Chemical studies on Chinese traditional medicine, dangshen. I. Isolation of (Z)-3- and (E)-2-hexenyl beta-D-glucosides. *Chem Pharm Bull (Tokyo)* 1988; **36**: 2689–90.
- 13 Nörr H, Wagner H. New constituents from *Codonopsis pilosula*. *Planta Med* 1994; **60**: 494–5.
- 14 Wong MP, Chiang TC, Chang HM. Chemical studies on Dangshen, the root of *Codonopsis pilosula*. *Planta Med* 1983; **49**: 60.
- 15 Chu X, Liu XJ, Qiu JM, Zeng XL, Bao HR, Shu J. Effects of *Astragalus* and *Codonopsis pilosula* polysaccharides on alveolar macrophage phagocytosis and inflammation in

- chronic obstructive pulmonary disease mice exposed to PM2.5. *Environ Toxicol Pharmacol* 2016; **48**: 76–84.
- 16 He JY, Ma N, Zhu S, Komatsu K, Li ZY, Fu WM. The genus *Codonopsis* (Campanulaceae): A review of phytochemistry, bioactivity and quality control. *J Nat Med* 2015; **69**: 1–21.
  - 17 Li Z, Zhu L, Zhang H et al. Protective effect of a polysaccharide from stem of *Codonopsis pilosula* against renal ischemia/reperfusion injury in rats. *Carbohydr Polym* 2012; **90**: 1739–43.
  - 18 Qin T, Ren Z, Lin D et al. Effects of selenizing *Codonopsis pilosula* polysaccharide on macrophage modulatory activities. *J Microbiol Biotechnol* 2016; **26**: 1358–66.
  - 19 Wang ZT, Ng TB, Yeung HW, Xu GJ. Immunomodulatory effect of a polysaccharide-enriched preparation of *Codonopsis pilosula* roots. *Gen Pharmacol* 1996; **27**: 1347–50.
  - 20 Xu C, Liu Y, Yuan G, Guan M. The contribution of side chains to antitumor activity of a polysaccharide from *Codonopsis pilosula*. *Int J Biol Macromol* 2012; **50** (4): 891.
  - 21 Yang C, Gou Y, Chen J, An J, Chen W, Hu F. Structural characterization and antitumor activity of a pectic polysaccharide from *Codonopsis pilosula*. *Carbohydr Polym* 2013; **98**: 886–95.
  - 22 Aslam SN, Newman MA, Erbs G et al. Bacterial polysaccharides suppress induced innate immunity by calcium chelation. *Curr Biol* 2008; **18**: 1078–83.
  - 23 Bates JM, Akerlund J, Mittge E, Guillemin K. Intestinal alkaline phosphatase detoxifies lipopolysaccharide and prevents inflammation in zebrafish in response to the gut microbiota. *Cell Host Microbe* 2007; **2**: 371–82.
  - 24 Nwodo UU, Green E, Okoh AI. Bacterial exopolysaccharides: Functionality and prospects. *Int J Mol Sci* 2012; **13**: 14002–15.
  - 25 Roca C, Alves VD, Freitas F, Reis MA. Exopolysaccharides enriched in rare sugars: Bacterial sources, production, and applications. *Front Microbiol* 2015; **6**: 288.
  - 26 Wang K, Li W, Rui X, Chen X, Jiang M, Dong M. Characterization of a novel exopolysaccharide with antitumor activity from *Lactobacillus plantarum* 70810. *Int J Biol Macromol* 2014; **63**: 133–9.
  - 27 Wu Z, Wang G, Pan D et al. Inflammation-related pro-apoptotic activity of exopolysaccharides isolated from *Lactococcus lactis* subsp. *lactis*. *Benef Microbes* 2016; **7**: 761–8.
  - 28 Matsuzaki C, Hayakawa A, Matsumoto K, Katoh T, Yamamoto K, Hisa K. Exopolysaccharides produced by *Leuconostoc mesenteroides* strain NTM048 as an immunostimulant to enhance the mucosal barrier and influence the systemic immune response. *J Agric Food Chem* 2015; **63**: 7009–15.
  - 29 Li W, Xia X, Tang W et al. Structural characterization and anticancer activity of cell-bound exopolysaccharide from *Lactobacillus helveticus* MB2-1. *J Agric Food Chem* 2015; **63**: 3454–63.
  - 30 Liu SB, Chen XL, He HL et al. Structure and ecological roles of a novel exopolysaccharide from the arctic sea ice bacterium *Pseudoalteromonas* sp. strain SM20310. *Appl Environ Microbiol* 2013; **79**: 224–30.
  - 31 Sungur T, Aslim B, Karaaslan C, Aktas B. Impact of exopolysaccharides (EPSs) of *Lactobacillus gasseri* strains isolated from human vagina on cervical tumor cells (HeLa). *Anaerobe* 2017; **47**: 137–44.
  - 32 Wang JS, Zhang Q, Cui F et al. Genome-wide analysis of gene expression provides new insights into cold responses in *Thellungiella salsuginea*. *Front Plant Sci* 2017; **8**: 713.
  - 33 Wang PF, Song H, Li CS et al. Genome-wide dissection of the heat shock transcription factor family genes in *Arachis*. *Front Plant Sci* 2017; **8**: 106.
  - 34 Zhao X, Leavitt SD, Zhao ZT et al. Towards a revised generic classification of lecanoroid lichens (Lecanoraceae, Ascomycota) based on molecular, morphological and chemical evidence. *Fungal Divers* 2016; **78**: 293–304.
  - 35 Zhu QL, Sun L, Lian JJ et al. The phospholipase C (*FgPLC1*) is involved in regulation of development, pathogenicity, and stress responses in *Fusarium graminearum*. *Fungal Genet Biol* 2016; **97**: 1–9.
  - 36 Feng ZT, Deng YQ, Zhang SC et al. K<sup>+</sup> accumulation in the cytoplasm and nucleus of the salt gland cells of *Limonium bicolor* accompanies increased rates of salt secretion under NaCl treatment using NanoSIMS. *Plant Sci* 2015; **238**: 286–96.
  - 37 Cao S, Du XH, Li LH et al. Overexpression of *Populus tomentosa* cytosolic ascorbate peroxidase enhances abiotic stress tolerance in tobacco plants. *Russ J Plant Physiol* 2017; **64**: 224–34.
  - 38 An J, Hou L, Li C et al. Cloning and expression analysis of four *DELLA* genes in peanut. *Russ J Plant Physiol* 2015; **62**: 116–26.
  - 39 Han G, Wang M, Yuan F, Sui N, Song J, Wang B. The CCCH zinc finger protein gene *AtZFP1* improves salt resistance in *Arabidopsis thaliana*. *Plant Mol Biol* 2014; **86**: 237–53.
  - 40 Guerrero R. Bergey's manuals and the classification of prokaryotes. *Int Microbiol* 2001; **4**: 103–9.
  - 41 Mailund T, Brodal GS, Fagerberg R, Pedersen CN, Phillips D. Recrafting the neighbor-joining method. *BMC Bioinformatics* 2006; **7**: 29.
  - 42 He CQ, Liu YX, Wang HM, Hou PL, He HB, Ding NZ. New genetic mechanism, origin and population dynamic of bovine ephemeral fever virus. *Vet Microbiol* 2016; **182**: 50–6.
  - 43 Ji W, Niu DD, Si HL, Ding NZ, He CQ. Vaccination influences the evolution of classical swine fever virus. *Infect Genet Evol* 2014; **25**: 69–77.
  - 44 Zhu YY, Xing WX, Shan SJ et al. Characterization and immune response expression of the Rig-I-like receptor mda5 in common carp *Cyprinus carpio*. *J Fish Biol* 2016; **88**: 2188–202.
  - 45 Bai B, Zhao J, Li Y et al. OsBBX14 delays heading date by repressing florigen gene expression under long and short-day conditions in rice. *Plant Sci* 2016; **247**: 25–34.
  - 46 Kaur G, Tirkey N, Bharrhan S, Chanana V, Rishi P, Chopra K. Inhibition of oxidative stress and cytokine

- activity by curcumin in amelioration of endotoxin-induced experimental hepatotoxicity in rodents. *Clin Exp Immunol* 2006; **145**: 313–21.
- 47 Yang Y, Mu T, Li T *et al.* Effects of FSTL1 on the proliferation and motility of breast cancer cells and vascular endothelial cells. *Thorac Cancer* 2017; **8**: 606–12.
- 48 Qin H, Zhou J, Zhou P *et al.* Prognostic significance of RelB overexpression in non-small cell lung cancer patients. *Thorac Cancer* 2016; **7**: 415–21.
- 49 Xie W, Yang Y, Gao S *et al.* The tumor suppressor CYLD controls epithelial morphogenesis and homeostasis by regulating mitotic spindle behavior and adherens junction assembly. *J Genet Genomics* 2017; **44**: 343–53.
- 50 Luo Y, Ran J, Xie S *et al.* ASK1 controls spindle orientation and positioning by phosphorylating EB1 and stabilizing astral microtubules. *Cell Discov* 2016; **2**: 16033.
- 51 Yang Y, Liu M, Li D *et al.* CYLD regulates spindle orientation by stabilizing astral microtubules and promoting dishevelled-NuMA-dynein/dynactin complex formation. *Proc Natl Acad Sci U S A* 2014; **111**: 2158–63.
- 52 Li D, Sun X, Zhang L *et al.* Histone deacetylase 6 and cytoplasmic linker protein 170 function together to regulate the motility of pancreatic cancer cells. *Protein Cell* 2014; **5**: 214–23.
- 53 Henneke P, Golenbock DT. Phagocytosis, innate immunity, and host-pathogen specificity. *J Exp Med* 2004; **199**: 1–4.
- 54 Schepetkin IA, Quinn MT. Botanical polysaccharides: Macrophage immunomodulation and therapeutic potential. *Int Immunopharmacol* 2006; **6**: 317–33.
- 55 Meng X, Yang DY, Li XD, Zhao SY, Sui N, Meng QW. Physiological changes in fruit ripening caused by overexpression of tomato SLAN2, an R2R3-MYB factor. *Plant Physiol Biochem* 2015; **89**: 24–30.
- 56 Song J, Shi WW, Liu RR *et al.* The role of the seed coat in adaptation of dimorphic seeds of the euhalophyte *Suaeda salsa* to salinity. *Plant Spec Biol* 2017; **32**: 107–14.
- 57 Song J, Zhou JC, Zhao WW *et al.* Effects of salinity and nitrate on production and germination of dimorphic seeds applied both through the mother plant and exogenously during germination in *Suaeda salsa*. *Plant Spec Biol* 2016; **31**: 19–28.
- 58 Liu SS, Wang WQ, Li M, Wan SB, Sui N. Antioxidants and unsaturated fatty acids are involved in salt tolerance in peanut. *Acta Physiol Plant* 2017; **39**: 207.
- 59 Zhao BT, Zhu XF, Jung JH, Xuan YH. Effect of brassinosteroids on ammonium uptake via regulation of ammonium transporter and N-metabolism genes in *Arabidopsis*. *Biol Plantarum* 2016; **60**: 563–71.
- 60 Liu M, Xie S, Zhou J. Use of animal models for the imaging and quantification of angiogenesis. *Exp Anim* 2018; **67**: 1–6.
- 61 Li H, Yang GW, Ma F *et al.* Molecular characterization of a fish-specific toll-like receptor 22 (TLR22) gene from common carp (*Cyprinus carpio* L.): Evolutionary relationship and induced expression upon immune stimulants. *Fish Shellfish Immunol* 2017; **63**: 74–86.
- 62 Zhao BT, Dai AH, Wei HC *et al.* *Arabidopsis* KLU homologue *GmCYP78A72* regulates seed size in soybean. *Plant Mol Biol* 2016; **90**: 33–47.
- 63 Li T, Li H, Peng SQ, Zhang FM, An LG, Yang GW. Molecular characterization and expression pattern of X box-binding protein-1 (XBP1) in common carp (*Cyprinus carpio* L.): Indications for a role of XBP1 in antibacterial and antiviral immunity. *Fish Shellfish Immunol* 2017; **67**: 667–74.
- 64 Liu TT, Yan JH. Review of the Palearctic *Atemelia* Herrich-Schaffer (Lepidoptera, Yponomeutoidea, Praydidae), with description of a new leafmining species. *Zootaxa* 2017; **4250**: 327–36.
- 65 Guo X, Zhao Y, Yan H *et al.* Single tumor-initiating cells evade immune clearance by recruiting type II macrophages. *Genes Dev* 2017; **31**: 247–59.
- 66 Zhou J, Qu Z, Sun F *et al.* Myeloid STAT3 promotes lung tumorigenesis by transforming tumor immunosurveillance into tumor-promoting inflammation. *Cancer Immunol Res* 2017; **5**: 257–68.
- 67 Sun S, Zhou J. Molecular mechanisms underlying stress response and adaptation. *Thorac Cancer* 2018; **9**: 218–27.
- 68 He X, Liu Z, He Q *et al.* Identification of novel microtubule-binding proteins by taxol-mediated microtubule stabilization and mass spectrometry analysis. *Thorac Cancer* 2015; **6**: 649–54.
- 69 Dehne N, Mora J, Namgaladze D, Weigert A, Brüne B. Cancer cell and macrophage cross-talk in the tumor microenvironment. *Curr Opin Pharmacol* 2017; **35**: 12–9.
- 70 Zheng X, Turkowski K, Mora J *et al.* Redirecting tumor-associated macrophages to become tumoricidal effectors as a novel strategy for cancer therapy. *Oncotarget* 2017; **8**: 48436–52.
- 71 Zhu B, Chen S, Wang H *et al.* The protective role of DOT1L in UV-induced melanomagenesis. *Nat Commun* 2018; **9**: 259.
- 72 Wang H, Zhang L, Yang L, Liu C, Zhang Q, Zhang L. Targeting macrophage anti-tumor activity to suppress melanoma progression. *Oncotarget* 2017; **8**: 18486–96.
- 73 Murray PJ, Allen JE, Biswas SK *et al.* Macrophage activation and polarization: Nomenclature and experimental guidelines. *Immunity* 2014; **41**: 14–20.
- 74 Dentan C, Lesnik P, Chapman MJ, Ninio E. Phagocytic activation induces formation of platelet-activating factor in human monocyte-derived macrophages and in macrophage-derived foam cells. Relevance to the inflammatory reaction in atherosclerosis. *Eur J Biochem* 1996; **236**: 48–55.
- 75 Grimes GR, Moodie S, Beattie JS *et al.* GPX-macrophage expression atlas: A database for expression profiles of macrophages challenged with a variety of pro-inflammatory, anti-inflammatory, benign and pathogen insults. *BMC Genomics* 2005; **6**: 178.
- 76 Yoon WJ, Kim SS, Oh TH, Lee N, Hyun CG. *Abies koreana* essential oil inhibits drug-resistant skin pathogen growth and LPS-induced inflammatory effects of murine macrophage. *Lipids* 2009; **44**: 471–6.